Development of a Pigment-Based Whole-Cell Zinc Biosensor for Human Serum

Daniel M. Watstein[ORCID] and Mark P. Styczynski*

School of Chemical & Biomolecular Engineering, Georgia Institute of Technology, 311 Ferst Drive NW, Atlanta, Georgia 30332-0100, United States

S *Supporting Information*

ABSTRACT: Deficiencies in vitamins and minerals (micronutrients) are a critical global health concern, in part due to logistical difficulties in assessing population micronutrient status. Whole-cell biosensors offer a unique opportunity to address this issue, with the potential to move sample analysis from centralized, resource-intensive clinics to minimal-resource, on-site measurement. Here, we present a proof-of-concept whole-cell biosensor in *Escherichia coli* for detecting zinc, a micronutrient for which deficiencies are a significant public health burden. Importantly, the whole-cell biosensor produces readouts (pigments) that are visible to the naked eye, mitigating the need for measurement equipment and thus increasing feasibility for sensor field-friendliness and affordability at a global scale. Two zinc-responsive promoter/transcription factor systems are used to differentially control production of three distinctly colored pigments in response to zinc levels in culture. We demonstrate strategies for tuning each zinc-responsive system to turn production of the different pigments on and off at different zinc levels, and we demonstrate production of three distinct color regimes over a concentration range relevant to human health. We also demonstrate the ability of the sensor cells to grow and produce pigment when cultured in human serum, the ultimate target matrix for assessing zinc nutritional status. Specifically, we present approaches to overcome innate immune responses that would otherwise hinder bacterial sensor survival, and we demonstrate production of multiple pigment regimes in human serum with different zinc levels. This work provides proof of principle for the development of low-cost, minimal-equipment, field-deployable biosensors for nutritional epidemiology applications.

KEYWORDS: *whole-cell biosensor, micronutrient deficiency, zinc assay, pigment readouts, serum, minimal equipment biosensor*
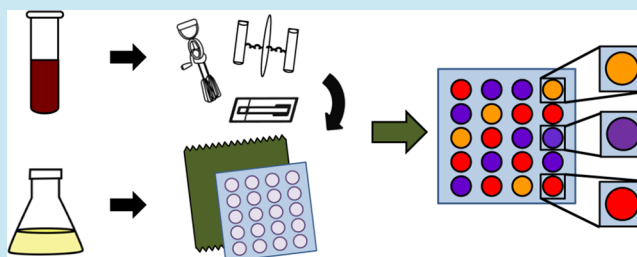
Nutritional deficiencies result in millions of deaths globally every year,[1] with the burden disproportionately borne by developing countries. A critical obstacle in addressing global malnutrition problems is the lack of detailed knowledge about which areas are most heavily affected by which nutritional deficiencies. This issue is particularly salient in the case of micronutrient deficiencies, often referred to as "hidden hunger" since people may appear to have sufficient food intake but are lacking appropriate levels of key vitamins and minerals (micronutrients). While aid agencies often use nutritional survey instruments (for example, food diaries or dietary recall) to estimate the intake of inhabitants of a given region, these methods can have limits on their accuracy due to, among other factors, discrepancies between varying local crop nutrient content and values in available databases[2,3] and bias of available information toward subgroups least at risk of deficiency.[4] The ideal approach to obtaining this data would be representative sampling and clinical measurement of circulating markers for nutritional status, but this is prohibitive on both logistical and economic grounds.[4] As such, the development of low-cost ways to measure nutritional markers in a logistically simplified fashion could have a significant impact on global health efforts, providing more detailed information on specific nutritional burdens in specific regions of the world and ultimately informing the efficient allocation of limited aid resources.

Whole-cell biosensors are a promising route for the creation of such inexpensive and simple ways to measure nutritional status. Microbes, as obligate consumers of a number of micronutrients, have evolved a wide array of transcription factors that differentially regulate genes in response to changes of nutrient levels in their environment. This existing cellular machinery could be leveraged to sense and report micronutrient levels in human biofluids at low cost. In addition, microbes can be programmed to produce reporters that are visible to the naked eye (e.g., pigments), which would minimize the need for sophisticated or expensive analytical equipment and thus enable low-cost, low-resource, portable measurement of micronutrient levels. An envisioned schematic for how an assay based on these methods might look is depicted in Figure 1a. Briefly, patient blood is taken in the field and separated on-site with innovative low-resource centrifuges (paper centrifuge,[5] egg-beater centrifuge[6]) or perhaps paper-based technology.[7] The resulting plasma is exposed to packaged, lyophilized cells.
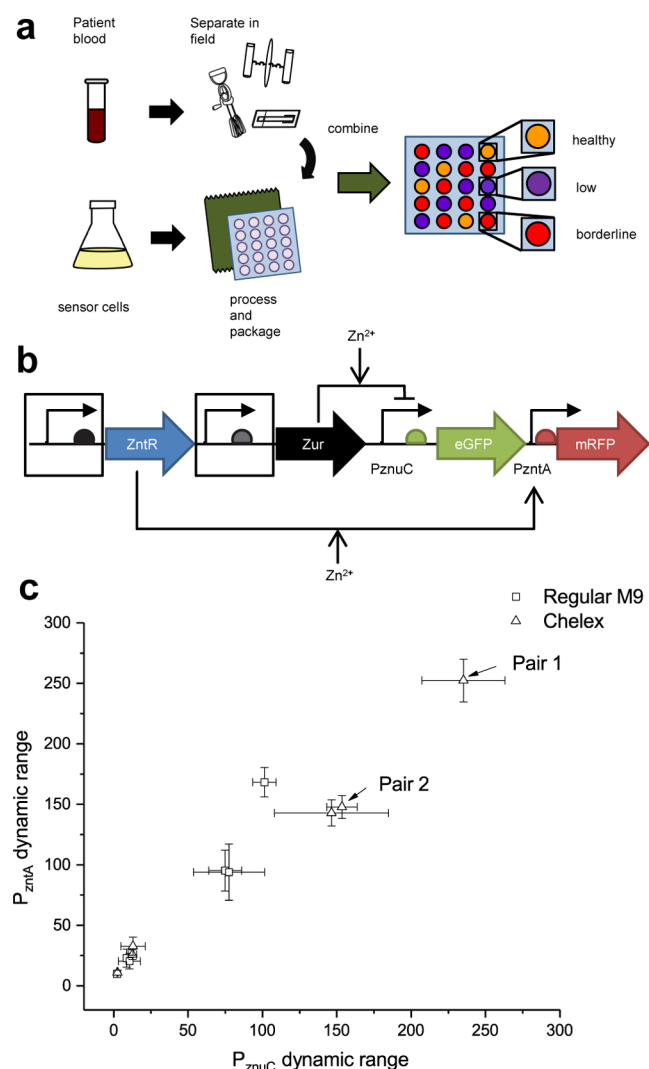
Figure 1. (a) Schematic of envisioned test implementation. Patient blood is collected in the field, separated using field-friendly approaches, and combined with packaged sensor cells. The cells grow and produce pigment indicative of subject micronutrient status. (b) Schematic of regulator test construct. The promoters and ribosomal binding sites (boxed) for zinc-responsive regulators ZntR and Zur were varied to determine optimal expression for improved dynamic range over physiologically relevant zinc concentrations. (c) Fluorescent reporter output demonstrating sensor dynamic range from 0 to 20 μM Zn^{2+} with different expression levels for ZntR and Zur. Regulator pairs one and two (arrows) were used in subsequent two- and three-color pigment biosensors. Error bars indicate standard deviation.

The whole-cell biosensor senses micronutrient levels and responds by producing pigmented metabolites (here, the red lycopene, orange β-carotene, and purple violacein), allowing for unambiguous, minimal-equipment determination of micronutrient status in the field. The work presented here focuses on the development of an assay for zinc levels.

Zinc is a critical micronutrient for human health, which has long been identified as a major public health burden in terms of contribution to nutritional deficiency burden and related morbidity and mortality.[1,8,9] Over 1 billion people across the world are at risk for zinc deficiency,[4] with at least 100 000 children under the age of 5 dying annually as a result of the problem and millions more experiencing its developmental and other deleterious effects.[8] The Biomarkers of Nutrition for Development (BOND) program identified zinc as one of the six key micronutrient deficiencies for which consensus on accurate assessment methodologies could have a major public health impact.[10] While treatable, a significant challenge in addressing zinc deficiency is its identification in populations in a more precise way than estimated dietary intake or food surveys,[11] yet in a more tractable way than traditional state-of-the-art testing of blood in a laboratory setting. Measuring serum zinc in the field as part of existing surveying efforts could be used to indicate population zinc status and guide policy-making decisions for zinc deficiency interventions.

Previous work in our lab was directed toward engineering the carotenoid pathway for more precise control of metabolism to allow for the zinc-responsive production of two pigments from one metabolic pathway. The zinc-responsive activator ZntR[12] and a cognate promoter, P_{zntA}, were used to allow cells to respond to changes in extracellular zinc. By altering ribosomal binding sites (RBSs) of carotenoid genes, adding protein degradation tags, controlling gene dosage though plasmid copy number, and increasing metabolic precursor availability through supplementation of the mevalonate pathway, stable zinc-responsive production of either lycopene or β-carotene from the same strain was enabled that represented intermediate and sufficient levels of zinc, respectively.[13] The challenge overcome in that work was eliciting this response over a fraction of ZntR/P_{zntA}'s natural dynamic range (0−1.1 mM)[14] that was closer to a physiologically relevant range found in human serum (3−16 μM).

Here, we present the results of our efforts to create a whole-cell sensor for zinc levels that uses multiple pigments as easy-to-read reporters. We integrate the production of three pigments into a single strain based on the zinc levels in which the cells are cultured. We expand upon our previously reported engineering efforts by optimizing regulator levels for increased dynamic range of promoters from 0 to 20 μM zinc, and we introduce a decoy-based tuning strategy for violacein expression under control of a second zinc-responsive system based on the promoter P_{znuC} and the zinc-responsive repressor Zur.[15] Finally, we demonstrate growth and proof-of-principle performance in human serum, which would ultimately be required for a device based on this biosensor.

■ RESULTS AND DISCUSSION

Dynamic Range of Promoter Regulator Pairs. In initial efforts, we identified that the expression levels of the zinc-responsive regulators ZntR and Zur can have a major impact on the dynamic range (ratio of maximum to minimum output over a given input range) of the promoters that they regulate (data not shown). Since a requisite step in our efforts is the precise engineering of metabolic state to enable production of (hopefully) only one pigment at a time,[16] a high dynamic range would enable a transition between repressed or uninduced levels of a pigment that are not visually detectable and induced levels that are obvious to the naked eye in a reasonable amount of time. We thus first sought to characterize the dynamic ranges of the two regulator/promoter systems at varying expression levels of the regulators.

To identify regulator expression levels that maximize the range of transcription rates available over a physiologically relevant concentration range of zinc, a series of fluorescent reporter plasmids was constructed consisting of transcriptionally insulated P_{zntA} and P_{znuC} controlling expression of mRFP

and eGFP. The regulators ZntR and Zur were constitutively expressed with different combinations of promoters and ribosomal binding sites (Figure 1b) of varying strength. These plasmids were transformed into *E. coli* and grown in minimal media with and without treatment by Chelex 100, a zinc-selective chelating resin, each with and without 20 μM supplemented ZnSO$_4$. Fluorescent output of both reporters was measured and compared to determine promoter performance over this range of zinc. The dynamic range of each promoter was calculated by taking the ratio of the largest to smallest fluorescence values of each promoter/regulator system at 0 and 20 μM ZnSO$_4$. The dynamic ranges of both promoter/regulator systems are plotted against each other in Figure 1c. The two highest dynamic range regulator pairs (referred to hereafter as Pair 1 and Pair 2) were selected for subsequent experiments with two- and three-pigment output sensors.

These efforts yielded some straightforward results as well as others that were not quite as expected. Unsurprisingly, most of the best performance was observed in the resin-treated media; both regulator systems already exhibit some degree of response (induction or repression) starting at low micromolar levels of zinc or below, so the trace levels of zinc present in untreated medium would cause greater baseline regulator activity in unsupplemented medium, ultimately yielding lower dynamic ranges for untreated versus Chelex-treated media. Interestingly, the regulator pairs that resulted in the highest dynamic ranges do not simply correspond to the highest expected regulator expression levels estimated by taking the product of the relative translation rate predicted by the Ribosomal Binding Site Calculator[17] and the previously characterized relative transcriptional output of constitutive promoters (Supporting Information Tables S1−S3). A possible explanation for this behavior is that the two regulators have different affinities for zinc and are both competing for zinc from the same pool.[18,19] Overexpression of these zinc-binding proteins likely affects the natural partitioning of zinc ions throughout the proteome. As a result, a change in expression of Zur could, for example, alter the availability of zinc for ZntR and thus change P$_{zntA}$ transcriptional output for a given concentration of zinc, even though Zur does not directly regulate P$_{zntA}$.

Two- and Three-Color Pigment Sensors. Using regulator levels from Pair 1 and Pair 2 from above, a library of pigment-based reporters was constructed with varying ribosomal binding strength and an LAA protein degradation tag[20] on *crtY*, the gene that converts lycopene to β-carotene, under control of P$_{zntA}$. (When plasmids are described here, they are identified by regulator pair and RBS on *crtY*, with 'L' denoting the presence of a degradation tag on *crtY*, such as Pair 1 33 or Pair 2 33L.) The lycopene operon from *Pantoea ananatis*, *crtEBI*, was constitutively expressed from a weak promoter. The library was grown at 0, 10, 20, and 100 μM zinc in minimal media for 24 h and carotenoids were extracted for HPLC analysis.

Figure 2a shows four representative library members demonstrating a variety of behavior over the tested zinc concentrations. First, at the two extrema, sensors were produced that were unable to appreciably respond to changes in zinc. In one case, the only accessible state at all tested zinc concentrations was β-carotene. This is a challenge in using two consecutive pigments in a metabolic pathway as reporters: tight control of downstream enzymes is necessary to maintain a color output of an intermediate metabolite, problems we previously found could be addressed by adjusting precursor availability.[13]
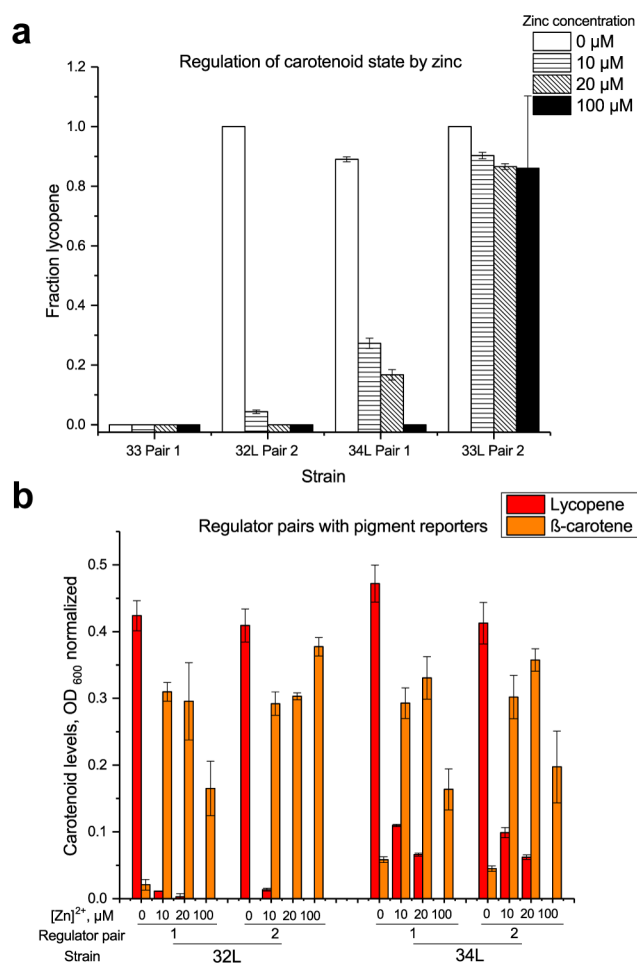

Figure 2. (a) Representative output of two-color biosensors showing two extreme cases in which sensor output does not switch (left, right) and two intermediate cases demonstrating a shift in concentration of zinc at which sensor switches from lycopene-dominated to β-carotene-dominated (middle). (b) Carotenoid output comparing regulator pairs. While a substantial difference between regulator pairs was observed with fluorescent reporters (Figure 1c), two different pigment reporters (32L and 34L) show different lycopene production behavior in response to zinc but little difference in carotenoid production as a function of regulator pair. Error bars indicate standard deviation.

This indicates that even with superior dynamic range from regulator Pair 1, leaky transcription from P$_{zntA}$ is still sufficient to prevent access to a lycopene-only state with a weak ribosomal binding site alone. At the other extreme, adding a degradation tag to *crtY* in concert with a weak ribosomal binding site is sufficient to prevent access to the β-carotene state. In between, stronger ribosomal binding sites coupled with a LAA degradation tag shift the switch point where cells become β-carotene dominated from between 0 and 10 μM Zn^{2+} (32L Pair 2) to between 20 and 100 μM Zn^{2+} (34L Pair 1), demonstrating that with these regulator pairs, precursor supplementation is not strictly necessary to switch states in the carotenoid pathway at these zinc levels. The degradation tag offers another potential opportunity to tune the effective dynamic range of the biosensor output; however, since we were primarily concerned with minimizing uninduced levels of CrtY in order to access the intermediate lycopene pigment state, only the strong LAA tag was used in this work.

A significant difference in fluorescent reporter output suggested that switching between regulator pairs one and two
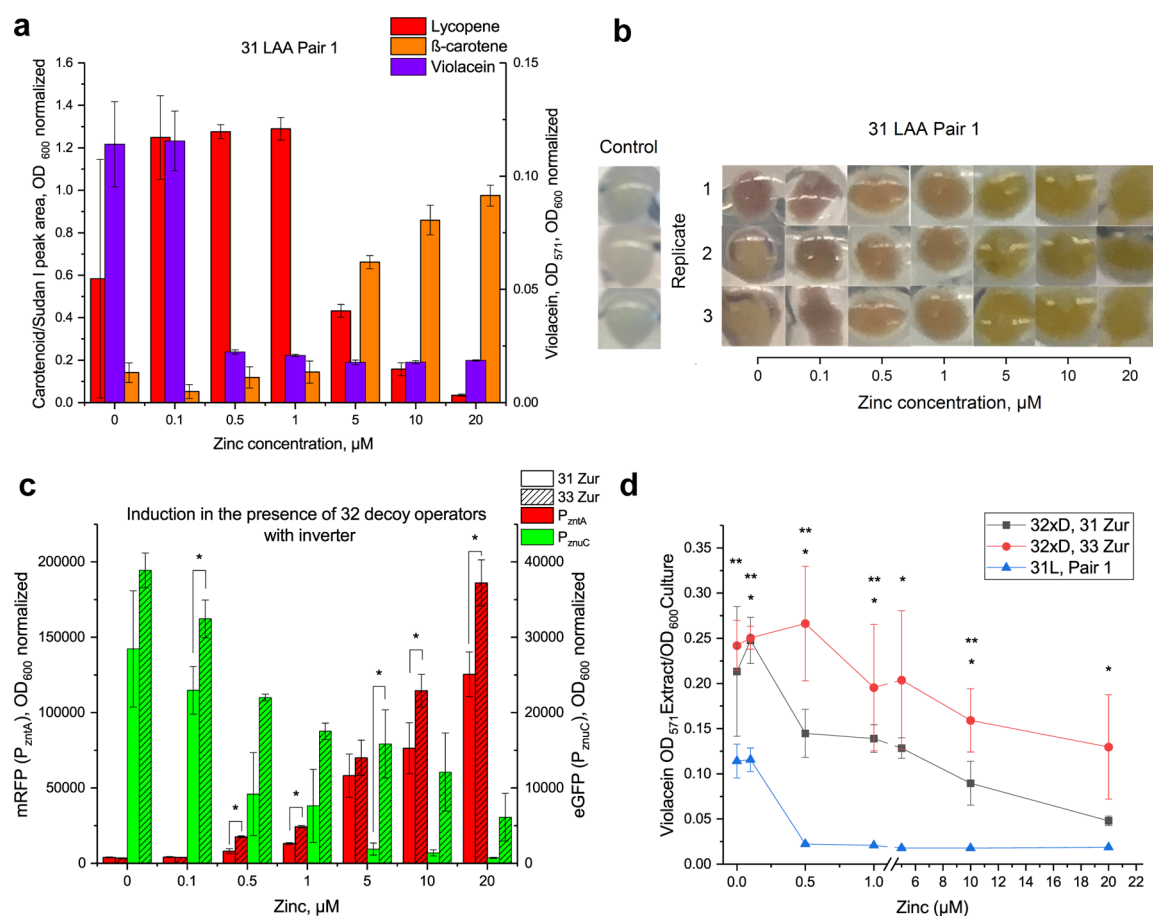
Figure 3. (a) Demonstration of a three-color sensor. At very low zinc, the cells produce substantial violacein and lycopene. At increasing concentrations of zinc, violacein production is repressed and the sensor is in a primarily lycopene state. As zinc increases further, lycopene is consumed and cells enter a primarily β-carotene state. (b) Cell pellets from the experiment in panel a. (c) Fluorescent reporter output in test with 32 decoy Zur operators and inducible Zur. Asterisks indicate significance at $p < 0.05$. (d) Violacein extract levels from decoy Zur operator test and varying RBS strength on inducible Zur. A construct without a decoy array or inducible Zur is presented for comparison (blue). Double asterisks denote statistical significance ($p < 0.05$) between red and blue. Single asterisks denote statistical significance between gray and blue ($p < 0.05$). Error bars indicate standard deviation.

would also allow fine-tuning of pigment control over the concentration range tested; however, two different pigment reporter constructs (32L and 34L) exhibited little to no change based on the regulator pair with which they were coupled (Figure 2b). In the case of 34L, no significant differences between the two regulator pairs were observed in lycopene and β-carotene measurements at any concentration range, including 10 and 20 μM Zn^{2+} at which there were intermediate amounts of both pigments. The 32L construct had significant differences in behavior of the two regulator pairs only at 100 μM and only in the total amount of β-carotene produced, as no lycopene was detected in either strain. This suggests that the response of the carotenoid pigment reporter is relatively robust to regulator expression levels. This was somewhat surprising, as we had previously observed that similar reporter constructs with genomic regulators alone or with genomic regulator operons coexpressed on the reporter plasmid were unable to switch state between lycopene and β-carotene and this was ameliorated by tuning regulator levels.

With the carotenoid reporter functioning over the desired concentration range in a few of the constructs, we selected the construct 31L Pair 1, which switched from a lycopene-dominated state to a β-carotene dominated state closer to 10 μM, for subsequent experiments. To 31L Pair 1, the second

zinc-responsive promoter, P$_{znuC}$, was added to control expression of the *vio* operon that produces the pigment violacein. This resulted in a strain that produced three distinct color states over a 20 μM Zn^{2+} concentration range (Figure 3a). At 0 and 0.1 μM Zn^{2+}, P$_{znuC}$ was derepressed and higher quantities of violacein were produced. At 0.5 and 1 μM Zn^{2+}, the sensor output was dominated by lycopene production. An intermediate state in which both lycopene and β-carotene were present in appreciable quantities was observed at 5 and 10 μM zinc, but by 20 μM zinc, the sensor output was dominated by β-carotene. The strategy in using these pigments was to tune violacein production to visually overpower lycopene in low zinc states such that the cells would appear purple even though lycopene was still present. In this construct, violacein production was not high enough at low zinc concentrations to produce a cell pellet in which only violacein was visibly detectable (Figure 3b); however, there remained a clear difference in pellet coloration between the high violacein states at low zinc and all other conditions. Additionally, though measured levels of both lycopene and β-carotene were intermediate at 5 and 10 μM zinc, there was little observable difference between the cell pellets from these conditions and those from 20 μM, at which essentially only β-carotene was

detected in appreciable quantities in extractions. The result of this is three distinct color states between 0 and 20 μM Zn^{2+}.

Some replicates with no supplemented zinc displayed some inhomogeneity in pigment production and formed a striated pellet in which cells with low or no violacein production formed the base of the pellet, making violacein difficult to detect visually (Figure 3b). Similar behavior was not observed at 0.1 μM. This behavior was not apparent in the extracts, as no substantial difference in normalized violacein production was measured at the two lowest zinc conditions (Figure 3a).

Tuning P$_{znuC}$ Response with Decoy Operators. Unfortunately, the concentration range at which violacein production becomes visually undetectable in the construct depicted in Figure 3a,b (less than 1 μM) is below medically relevant levels in human serum. To address this issue, we explored the use of additional "decoy" binding sites to sequester zinc-bound Zur and thus increase the zinc concentration necessary to yield sufficient zinc-bound Zur to repress expression of the violacein operon. We introduced to the plasmid an array of eight decoy binding sites for Zur comprising a combination of P$_{zinT}$[21] operators and completely palindromic P$_{znuC}$ operators. On a fluorescent reporter construct for P$_{zntA}$ and P$_{znuC}$ with no additional regulator expression (only genomic expression), the decoy array had the effect of significantly increasing the levels of the fluorescent reporter under full zinc repression, but it did not significantly alter (Supporting Information Figure S1) the zinc concentration at which expression first reached its minimum.

In an attempt to rectify this, the number of decoy binding sites was increased to 32 and *zur* was placed under the control of P$_{zntA}$ with either a weak (33) or intermediate strength (31) ribosomal binding site (Figure 3c), decreasing Zur levels at low zinc concentrations. Induction from 0 to 20 μM produced higher P$_{znuC}$ output in the reporter with the weaker RBS for Zur compared to the stronger RBS at all zinc concentrations, though these differences were only significant ($p < 0.05$) at 0.1 and 5 μM Zn^{2+}. This is consistent with the hypothesis that driving expression of Zur from P$_{zntA}$ yields insufficient Zur at low zinc concentrations to saturate the decoy array and P$_{znuC}$. As transcription from P$_{zntA}$ increases with Zn^{2+} concentration, additional Zur is produced, further repressing P$_{znuC}$ (though with the weaker RBS, there is still insufficient Zur to fully repress fluorescence). P$_{zntA}$ output was also increased significantly at all concentrations except 0, 0.1, and 5 μM Zn^{2+} ($p < 0.05$). The interpretation of this is less straightforward, but a possibility is that for any given concentration of zinc, there should be less Zur expressed from plasmids with the weaker RBS and thus fewer molecules to compete with constant ZntR levels for zinc binding. Though this strategy no longer relies directly on the natural dynamics of zinc binding to Zur to regulate P$_{znuC}$, these results demonstrate that the decoy array and inducible expression of the repressor are effective at shifting the apparent concentration at which expression from P$_{znuC}$ is fully repressed from about 0.3 μM (no decoys and regulator Pair 1, data not shown) to between 1 and 5 μM (32 decoys with strong RBS on Zur) to greater than 20 μM (32 decoys and weak RBS on Zur). This suggests that the threshold between sensor color output for a given strain can be effectively tuned based on the final needs of the sensor using this approach.

The same changes were made to the pigment reporter construct. Violacein extractions (Figure 3d) and cell pellets (Supporting Information Figure S2) both show trends similar

to those seen with the fluorescent reporter. The violacein content of strains with the stronger RBS on *zur* was significantly higher at all zinc concentrations above zero, and the weaker RBS was significant under all conditions except 5 and 20 μM Zn^{2+} (while the trends were consistent, increased variability brought the differences below $p < 0.05$). Though the strain harboring the weaker RBS had more violacein on average, the difference between the two decoy strains was not statistically significant at any concentration of zinc. These results demonstrate that behavior of the decoy array and inducible repressor is replicated using pigments, meaning that the concentrations at which violacein becomes undetectable and thus the sensor color output changes can be effectively tuned using this approach.

A likely source of variance in the violacein measurements is instability in the decoy array. We observed significant loss of violacein pigmentation in biological replicates during some experiments and suspected that the decoy array might be altered in cultures exhibiting that behavior due to the number and proximity of repeated nucleotide sequences in the decoy array and the high cellular strain of enzyme expression. To assess this, plasmid DNA from a sample of the cultures was amplified using PCR, showing significant deviations from the expected band length (Supporting Information Figure S3) and frequently revealing an assortment of decoy array lengths. Though the presence of repeated sequences on a plasmid might be inherently unstable, we note that we only observed this phenomenon in plasmids using pigments as reporters. Since loss of decoy sites would significantly reduce expression of the *vio* operon, this observation suggests that violacein expression is a significant burden on cells and such deletions are probably selected for evolutionarily, putting practical limits on the number of decoy sites possible in arrays.

Growth and Testing in Serum. Ultimately, the application of a field-deployable biosensor will require the direct measurement of a common biofluid. For zinc, this necessitates biosensor growth and/or response in human serum or plasma. One of the prevailing recommendations for evaluating zinc status is plasma zinc,[10] but to facilitate development, we chose to use pooled commercial off-the-clot serum to avoid any potential interference from coagulants or anticoagulants. While there is a potential discrepancy between serum and plasma zinc levels, this is solely due to how the fluids are commonly handled prior to analysis, and choosing serum zinc allowed us to evaluate the sensor in a similar matrix to what would be expected in the field.[10] To simulate zinc deficiency, the serum was treated with Chelex 100 resin to remove zinc, allowing retitration to measure the response of the sensor at various concentrations of zinc.

In initial experiments, cultures were inoculated with small volumes of resuspended colonies from agar plates. We grew these in mixtures of serum and media with increasing percentages of serum, but we were unable to grow cultures in even our lowest (10%) serum concentration (data not shown). This interference with bacterial growth may have been due to the passive immune functionality present in human serum in the form of the complement system,[22] a cascade of proteins with the ability to form pores in foreign cell membranes, ultimately causing lysis.

To test if something similar to complement system protein activity in serum was interfering with growth, we compared cultures with low percentages of normal human serum (NHS), heat-inactivated normal human serum (HI NHS), and fetal
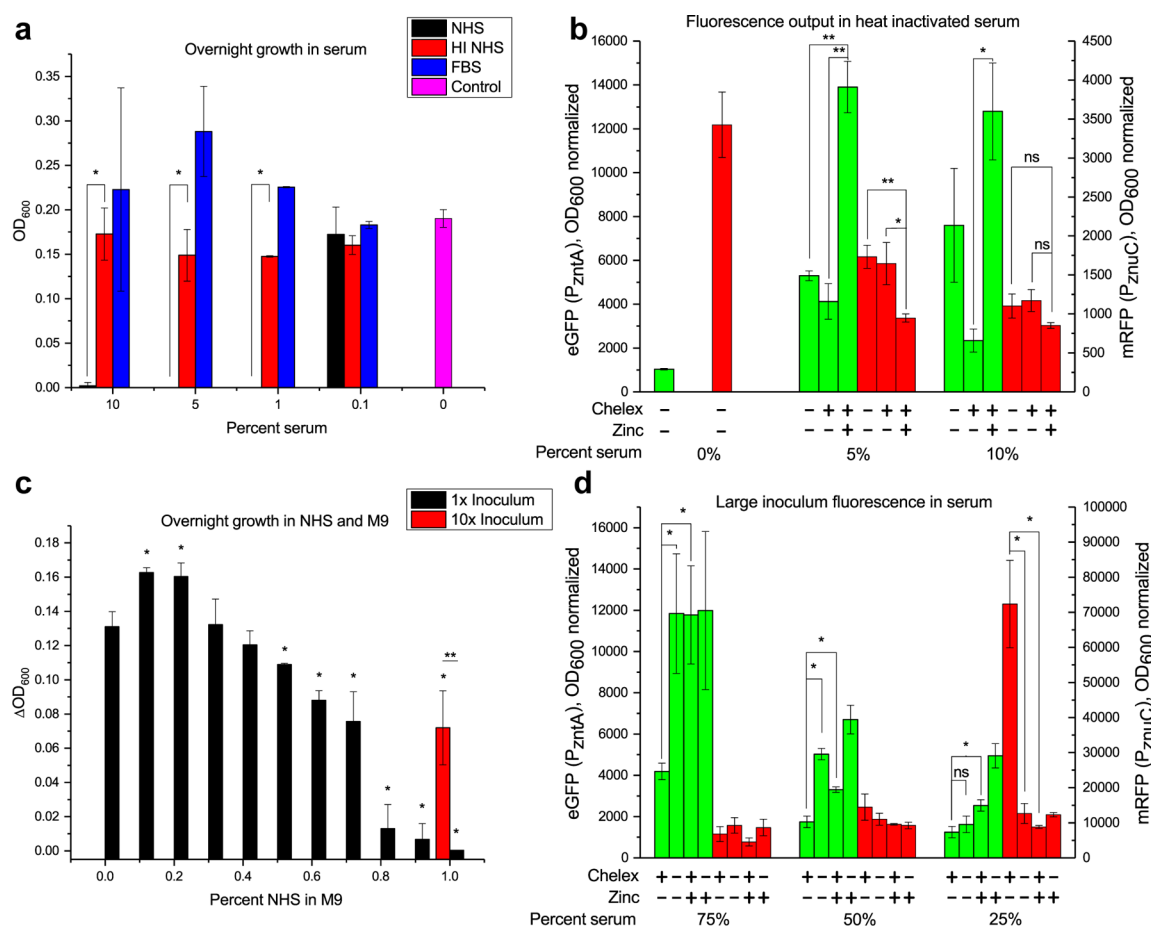
Figure 4. (a) Growth of DH10B in decreasing concentrations of normal human serum (NHS), heat-inactivated human serum, and fetal bovine serum. Normal human serum cultures failed to grow at all concentrations above 0.1%. Asterisks indicate differences at $p < 0.05$. (b) Fluorescent reporter demonstrating sensor response in heat-inactivated human serum treated with Chelex 100 resin. At 5% serum, differences were significant between cultures with and without zinc supplementation for both P_{znuC} and P_{zntA} (** $p < 0.01$, * $p < 0.05$). Zinc supplemented as if serum had 10 μM zinc. (c) NHS titration in M9. 10× inoculum only used at 1% NHS experimental condition (* $p < 0.05$ compared to 0, ** $p < 0.05$ compared to 10× inoculum). (d) Large-inoculum test of fluorescent reporter in human serum (* $p < 0.05$). Zinc supplemented as if serum had 5 μM zinc. Specific statistical comparisons relevant for discussions in the text are highlighted; lack of a comparison does not indicate lack of significant differences. Error bars indicate standard deviation.

bovine serum (FBS) that had not been heat-inactivated. Heat inactivation should render the complement system or similar protein actors inactive and prevent lysis of the biosensor; although FBS should have some form of a complement system, it should have lower levels of complement than adult serum.[23] DH10B grew robustly in all tested concentrations below 10% in both HI NHS and FBS but only at 0.1% NHS (Figure 4a), suggesting that the complement system or something similar interferes with cell growth.

To test sensor response, we compared our fluorescent reporter in HI NHS, Chelex-treated HI NHS, and zinc-supplemented resin-treated serum (Figure 4b). We achieved robust growth up to 10% serum under all conditions, but none at 50% serum. (While a standard protocol was used for heat inactivation, it is likely that the complement system was not completely inactivated in these experiments as growth was observed in higher percentage serum in subsequent experiments.) The difference in fluorescent reporter output was statistically significant ($p < 0.05$) between Chelex-treated and 10 μM supplemented Chelex-treated serum at 5% for P_{znuC} and at both 5 and 10% for P_{zntA}, indicating that both promoter/regulator pairs could detect changes in a physiologically relevant zinc concentration in low-percentage serum media.

The lack of significant difference in P_{znuC} output observed with and without the addition of zinc could be due to an incomplete removal of zinc by the commercial resin. P_{znuC} and Zur respond below 0.5 μM in minimal media, and a small amount of zinc remaining in serum could cause the discrepancy between 5 and 10% serum media.

Since achieving consistent and inexpensive heat inactivation in the field poses significant challenges, we investigated alternative methods of achieving growth in NHS. Since growth was observed in initial serum experiments at 0.1%, we sought to identify at what percentage serum the culture growth becomes significantly reduced and if this was dependent on the initial inoculum. Titrating serum down in 0.1% increments from 1%, we saw significant growth below 0.7% NHS (Figure 4c) with significantly increased growth relative to no serum at 0.2 and 0.1%. Additionally, a 10-fold increase in inoculum achieved growth in 1% serum, suggesting that it may be possible to simply overwhelm the complement system with a sufficient bacterial inoculum.

To further investigate the potential for using high inoculation density to overcome growth limitations due to the complement system, overnight cultures were grown, pelleted, and concentrated in small volumes of media (OD_{600}: 68). Different

volumes of the resuspension were inoculated in 96-well plates in 100 and 50% normal human serum in M9 media. After incubation for 24 h, there was a clear cutoff between a starting OD_{600} of 0.227 (0.5 μL inoculum) and 0.0612 (0.135 μL inoculum) in 50% NHS (Supporting Information Figure S4). Only higher inoculum volumes were used in 100% NHS, and all conditions had positive changes in OD_{600}; however, optical density changes were significantly lower in 100% serum compared to 50%.

To determine appropriate serum conditions to test response of the biosensor, the fluorescent reporter was inoculated in 75, 50, and 25% NHS and Chelex-treated NHS with and without supplemented zinc (Figure 4d). The fluorescence readings of P_{zntA} could differentiate between NHS and Chelex-treated NHS without zinc and between Chelex-treated NHS with and without zinc at both 75 and 50% serum by volume ($p < 0.05$). At 25% serum, the fluorescence readings could differentiate between Chelex-treated NHS with and without zinc, but differences between NHS and Chelex-treated NHS without zinc were not significant. Results for P_{znuC} fluorescent output yielded the opposite results, with detectable differences between NHS and Chelex-treated NHS and between Chelex-treated NHS with and without zinc supplementation at 25% only ($p < 0.05$).

As the most significant challenge with the three-color pigment system is sufficiently precise tuning of the highly zinc sensitive Zur/P_{znuC} system, 25% serum was used to test the sensor response in human serum. A starter culture with pigment reporter plasmid harboring a 32× Zur operator decoy array and an intermediate strength RBS on *zur* was concentrated as described above, inoculated at a starting OD_{600} of 0.325, and grown for 24 h in 25% NHS and Chelex-treated serum with varying levels of zinc supplementation. Extracts (Figure 5a) and cell pellets (Figure 5b) demonstrate a high violacein and lycopene state at the lowest zinc concentration. All higher-zinc conditions have a mixture between lycopene and β-carotene and decreasing expression of violacein, showing the sensor in transition between carotenoid states. Violacein production is substantial under all conditions except for untreated NHS. Since pooled commercial NHS should contain healthy zinc levels, these results clearly indicate that more tuning of the carotenoid transition point will be necessary (which we have demonstrated here and in previous work[13]); however, it is extremely promising that violacein production has dropped to a level such that it is not visible in cell pellets at healthy zinc levels (Figure 5b, left).

Notably, violacein production is significantly higher at low zinc conditions in 25% serum than in M9 alone (compare Figure 5a to Figure 3d), and a large fraction of violacein is found in the supernatant of serum cultures. This could be due to metabolic changes in *E. coli* induced by human serum. Another explanation is that since violacein preferentially partitions into the media when serum is present, intracellular levels of violacein are kept lower in serum cultures than in M9 alone. A possible explanation for increased violacein in serum-containing media is solubilization of violacein by interaction with serum proteins (most likely human serum albumin) or perhaps lipids. Removal of product from the cells due to increased solubility in the media could help pull on the metabolic pathway and/or prevent intracellular violacein toxicity. Supernatants from M9 cultures show no visible violacein retention, though small differences in absorbance are detectable between butanol extractions of supernatant from
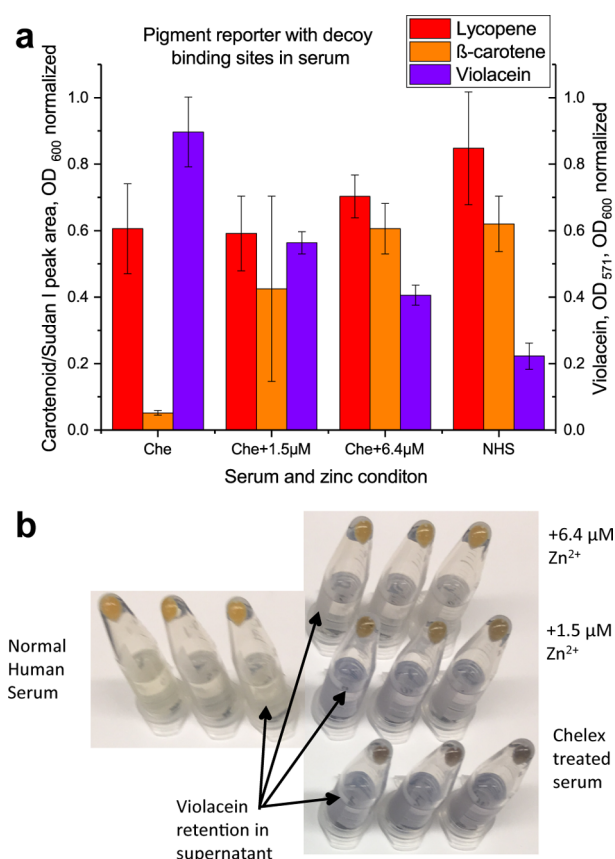

Figure 5. (a) Extract from biosensor culture in 25% NHS. Chelex-treated serum exhibits violacein-dominated low zinc output. NHS is characteristic of output in a healthy individual. (b) Cell pellets from 1 mL of 24 h culture of biosensor in 25% serum. Zinc supplementation levels were selected to mimic NHS. Here, NHS (left) shows characteristic pigment output of sensor in the presence of healthy zinc levels from commercial pooled serum. Chelex 100-treated serum (right) shows pigment output characteristic of low zinc to intermediate zinc states.

cultures with cells harboring different amounts of violacein. Cell pellets from M9 cultures were observed to contain more violacein than those in 25% serum, even as total violacein production in serum cultures was significantly greater as assessed by measurement of violacein in the supernatant (Supporting Information Figure S5).

■ CONCLUSIONS

In summary, we have demonstrated a proof-of-concept whole-cell biosensor that produces outputs detectable and interpretable by the naked eye at physiologically relevant zinc levels in 25% human serum. By optimizing expression levels of regulators for improved dynamic range of P_{zntA}/ZntR and P_{znuC}/Zur between 0 and 20 μM Zn^{2+}, we demonstrated the ability to tune the sensor output between the carotenoids lycopene and β-carotene to indicate borderline and healthy zinc levels. A strategy to adjust the response of P_{znuC}, initially occurring at nonphysiologically low concentrations of zinc, was demonstrated using arrays of decoy binding sites for Zur and using P_{zntA} output to control Zur, fully repressing it at zinc levels found in healthy serum and allowing violacein expression at levels expected to be physiologically relevant. Interference with sensor cell growth in human serum by the complement system or something similar was overcome via high-density

inoculations, and a proof-of-concept test of a three-color sensor was presented. The final transition thresholds between purple, red, and orange for a final field-deployed device cannot be determined now, as they will ultimately depend on the final form factor and assay protocol (e.g., percentage serum) of a field-friendly packaged and preserved device (which is the subject of ongoing efforts). Our proof-of-principle presented here for the sensor—demonstrating three color regimes in media cultures and the ability to produce the same pigments in serum culture—combined with our demonstrated ability to tune those transition thresholds suggests that whatever the final desired thresholds may be will be readily achievable using the tools and approaches demonstrated here.

■ METHODS

Plasmids and Oligonucleotides. Plasmids and primers from this work appear in Supporting Information Tables. Oligonucleotide synthesis and sequence verification of all constructed plasmids were performed by Eurofins Genomics.

Molecular Biology. All enzymes were purchased from New England Biolabs. PCR amplification was performed with Q5 polymerase. Plasmids were constructed with standard restriction endonuclease cloning or Gibson assembly.[24] All experiments used the *E. coli* strain DH10B. For routine cloning, cultures were grown in LB supplemented as necessary with chloramphenicol, tetracycline HCl, and kanamycin sulfate at final concentrations of 33, 15, and 50 μg/mL, respectively. Plasmid purification was performed with (Omega) kits. Purification of PCR products was performed with Qiagen kits.

Zur Decoy Array Construction. To construct the array of decoy Zur operators, oligonucleotides were synthesized containing portions of a modified palindrome and the Zur operator site in P_{ZinT} and appropriate restriction sites with sufficient overlapping sequences. These oligonucleotides were mixed and extended with Q5 polymerase (New England Biolabs) to create double stranded DNA, which was purified with a Qiaquick PCR purification kit (Qiagen), digested, and cloned into vectors to convert them to standard BioBrick format. These were then serially cloned to produce the 8× and 32× decoy arrays.

Violacein Extraction. One milliliter of culture was centrifuged for 5 min at 17 900 rcf. The supernatant was decanted, 50 μL of deionized water was added, and the pellets were vortexed for 5 min in a VWR VX-2500 multitube vortexer on the maximum speed setting. 250 μL of water-saturated butanol was added, and tubes were vortexed for an additional 5 min. Butanol suspensions were centrifuged for 5 min at 17 900 rcf, and the organic phase was transferred to fresh tubes and centrifuged again. The supernatant was transferred into microcuvettes and measured in a Genesys 20 spectrophotometer for absorbance at 571 nm using water-saturated butanol as a blank. For serum cultures and select M9 cultures, an additional measurement of the supernatant was taken for absorbance at 571 nm.

Acetone Extraction. Cultures were centrifuged and resuspended as above, and then mixed with 800 μL of acetone at 50 °C to which 1 μg/mL Sudan I had been added as an internal standard. Tubes were agitated regularly for 10 min and then centrifuged at 17 900 rcf for 5 min. 450 μL of the extract was transferred to autosampler vials for HPLC analysis. Vials were stored at −80 °C until analysis for no more than 24 h.

Carotenoid Analysis. HPLC analysis was performed on a Shimadzu Prominence UFLC with a UV−vis detector.

Separation was done on an Agilent Zorbax Extend-C18 Analytical 4.6 × 50 mm 5-μm column. Mobile phase composition was 50:30:20 methanol/acetonitrile/isopropanol at a flow rate of 1 mL/min. Peaks were identified by comparison with standards purchased from Sigma (lycopene, ≥ 90%) and TCI America (β-carotene, 97%). Reported carotenoid levels were calculated from the ratios of carotenoid peak areas with Sudan I peak areas normalized by the OD_{600} of the source culture.

Chelex 100 Treatment. When indicated, materials were treated with pH-corrected Chelex 100 resin (Biorad) using the manufacturer's batch protocol. Following treatment with Chelex resin, media were filter sterilized with 0.2 μm filters.

Modified M9 Media. A modified minimal medium similar to M9 except with organic phosphate to allow zinc titration was used for all experiments in minimal medium. A 5× salt solution was made containing 10 g/L β-glycerophosphate, 8.2 g/L KCl, 22.5 g/L NaCl, 5 g/L NH_4Cl, and 19.5 g/L MES, which was adjusted to pH 7.4. The salt solution was combined with 1.92 g of SC-ura amino acid mixture (Sunrise Science), 2 mL of 1 M $MgSO_4$, 100 μL of 1 M $CaCl_2$, 5 mL of 80% glycerol, 10 mL of 20% glucose, and 10 mL of 1% Thiamine HCl, diluted to a final volume of 1L, and filter sterilized.

Cell Culture. All cultures were inoculated from freshly transformed DH10B colonies. For minimal media and small-inoculum serum experiments, colonies were resuspended in 52 μL of M9. Five milliliter cultures were inoculated with 3 μL of these resuspensions. For large-inoculum serum experiments, six 8 mL overnight feeder cultures were grown in M9 with 1 μM supplemented $ZnSO_4$ and resuspended in a volume of 400 μL of M9. The optical density of a serial dilution of the resuspension was used to determine inoculum volumes. Cultures were grown aerobically for 24 h at 37 °C. For fluorescence experiments, optical density measurements and fluorescence readings were taken on a Synergy H4 (Biotek) plate reader using 150 μL aliquots of cultures in 96-well plates.

■ ASSOCIATED CONTENT

Ⓢ Supporting Information

The Supporting Information is available free of charge on the ACS Publications website at DOI: 10.1021/acssynbio.7b00292.

Effect of decoy Zur operators on the output of P_{znuC}; cell pellets from the violacein extraction experiment described in Figure 3d; characteristic banding pattern of CPCR of cells taken from a 32× decoy pigment induction experiment; overnight changes in OD in 100 and 50% serum in plates initial ODs; comparison of images of cell pellets and culture supernatants from three color experiments in 25% serum versus M9 alone; rank order lists of top fluorescent reporter dynamic ranges; output from RBScalc and relative transcriptional strength of promoters; description of files containing plasmid insert sequences; lists of genetic components and primers used in this study; sequences of vectors used in this study (PDF)

Compressed archive of annotated nucleic acid sequences describing the constructs used in this work (ZIP)

■ AUTHOR INFORMATION

Corresponding Author

*E-mail: Mark.Styczynski@chbe.gatech.edu.

ORCID

Daniel M. Watstein: 0000-0003-0872-8795

■ REFERENCES

(1) Black, R. E., Allen, L. H., Bhutta, Z. A., Caulfield, L. E., de Onis, M., Ezzati, M., Mathers, C., and Rivera, J. (2008) Maternal and child undernutrition: global and regional exposures and health consequences. *Lancet 371*, 243−260.

(2) Verma, D. K., and Srivastav, P. P. (2017) Proximate Composition, Mineral Content and Fatty Acids Analyses of Aromatic and Non-Aromatic Indian Rice. *Rice Science 24*, 21−31.

(3) Kennedy, G., and Burlingame, B. (2003) Analysis of food composition data on rice from a plant genetic resources perspective. *Food Chem. 80*, 589−596.

(4) Wessells, K. R., and Brown, K. H. (2012) Estimating the Global Prevalence of Zinc Deficiency: Results Based on Zinc Availability in National Food Supplies and the Prevalence of Stunting. *PLoS One 7*, e50568.

(5) Bhamla, M. S., Benson, B., Chai, C., Katsikis, G., Johri, A., and Prakash, M. (2017) Hand-powered ultralow-cost paper centrifuge. *Nature Biomedical Engineering 1*, 0009.

(6) Wong, A. P., Gupta, M., Shevkoplyas, S. S., and Whitesides, G. M. (2008) Egg beater as centrifuge: isolating human blood plasma from whole blood in resource-poor settings. *Lab Chip 8*, 2032−2037.

(7) Yang, X., Forouzan, O., Brown, T. P., and Shevkoplyas, S. S. (2012) Integrated separation of blood plasma from whole blood for microfluidic paper-based analytical devices. *Lab Chip 12*, 274−280.

(8) Black, R. E., Victora, C. G., Walker, S. P., Bhutta, Z. A., Christian, P., de Onis, M., Ezzati, M., Grantham-McGregor, S., Katz, J., Martorell, R., and Uauy, R. (2013) Maternal and child undernutrition and overweight in low-income and middle-income countries. *Lancet 382*, 427−451.

(9) Brown, K. H., Rivera, J. A., Bhutta, Z., Gibson, R. S., King, J. C., Lonnerdal, B., Ruel, M. T., Sandtrom, B., Wasantwisut, E., and Hotz, C. (2004) Assessment of the risk of zinc deficiency in populations and options for its control. *Food Nutr. Bull. Suppl.*, S94−S203.

(10) King, J. C., Brown, K. H., Gibson, R. S., Krebs, N. F., Lowe, N. M., Siekmann, J. H., and Raiten, D. J. (2016) Biomarkers of Nutrition for Development (BOND)-Zinc Review. *J. Nutr. 146*, 858S−885S.

(11) Hess, S. Y., Peerson, J. M., King, J. C., and Brown, K. H. (2007) Use of serum zinc concentration as an indicator of population zinc status. *Food Nutr. Bull. 28* (28), S403−S429.

(12) Outten, C. E., Outten, F. W., and O'Halloran, T. V. (1999) DNA distortion mechanism for transcriptional activation by ZntR, a Zn(II)-responsive MerR homologue in Escherichia coli. *J. Biol. Chem. 274*, 37517−37524.

(13) Watstein, D. M., McNerney, M. P., and Styczynski, M. P. (2015) Precise metabolic engineering of carotenoid biosynthesis in Escherichia coli towards a low-cost biosensor. *Metab. Eng. 31*, 171−180.

(14) Brocklehurst, K. R., Hobman, J. L., Lawley, B., Blank, L., Marshall, S. J., Brown, N. L., and Morby, A. P. (1999) ZntR is a Zn(II)-responsive MerR-like transcriptional regulator of zntA in Escherichia coli. *Mol. Microbiol. 31*, 893−902.

(15) Patzer, S. I., and Hantke, K. (2000) The zinc-responsive regulator Zur and its control of the znu gene cluster encoding the ZnuABC zinc uptake system in Escherichia coli. *J. Biol. Chem. 275*, 24321−24332.

(16) McNerney, M. P., Watstein, D. M., and Styczynski, M. P. (2015) Precision metabolic engineering: The design of responsive, selective, and controllable metabolic systems. *Metab. Eng. 31*, 123−131.

(17) Espah Borujeni, A., Channarasappa, A. S., and Salis, H. M. (2014) Translation rate is controlled by coupled trade-offs between site accessibility, selective RNA unfolding and sliding at upstream standby sites. *Nucleic Acids Res. 42*, 2646−2659.

(18) Outten, C. E., and O'Halloran, T. V. (2001) Femtomolar sensitivity of metalloregulatory proteins controlling zinc homeostasis. *Science 292*, 2488−2492.

(19) Wang, D., Hosteen, O., and Fierke, C. A. (2012) ZntR-mediated transcription of zntA responds to nanomolar intracellular free zinc. *J. Inorg. Biochem. 111*, 173−181.

(20) McGinness, K. E., Baker, T. A., and Sauer, R. T. (2006) Engineering Controllable Protein Degradation. *Mol. Cell 22*, 701−707.

(21) Gilston, B. A., Wang, S., Marcus, M. D., Canalizo-Hernández, M. A., Swindell, E. P., Xue, Y., Mondragón, A., and O'Halloran, T. V. (2014) Structural and Mechanistic Basis of Zinc Regulation Across the E. coli Zur Regulon. *PLoS Biol. 12*, e1001987.

(22) Dunkelberger, J. R., and Song, W. C. (2010) Complement and its role in innate and adaptive immune responses. *Cell Res. 20*, 34−50.

(23) Linscott, W. D., and Triglia, R. P. (1981) The bovine complement system. *Adv. Exp. Med. Biol. 137*, 413−430.

(24) Gibson, D. G., Young, L., Chuang, R.-Y., Venter, J. C., Hutchison, C. A., and Smith, H. O. (2009) Enzymatic assembly of DNA molecules up to several hundred kilobases. *Nat. Methods 6*, 343−345.